Size-resolved cloud condensation nuclei concentration measurements in the Arctic: two case studies from the summer of 2008

J. Zábori[1], N. Rastak[1], Y. J. Yoon[2], I. Riipinen[1], J. Ström[1]

[1]{Department of Environmental Science and Analytical Chemistry, Stockholm University, 106 91 Stockholm, Sweden}

[2]{Korea Polar Research Institute, Incheon 406-840, Republic of Korea}

Correspondence to: J. Zábori (julia.zabori@aces.su.se)

Abstract

The Arctic is one of the most vulnerable regions affected by climate change. Extensive measurement data are needed to understand the atmospheric processes governing this vulnerability. Among these, data describing cloud formation potential are of particular interest, since the indirect effect of aerosols on the climate system is still poorly understood. In this paper we present, for the first time, size-resolved cloud condensation nuclei (CCN) data obtained in the Arctic. The measurements were conducted during two periods in the summer of 2008: one in June, and one in August, at the Zeppelin research station (78°54'N, 11°53'E) in Svalbard. Trajectory analysis indicates that during the measurement period in June 2008, air masses predominantly originated from the Arctic, whereas the measurements from August 2008 were influenced mid-latitude air masses. CCN supersaturation (SS) spectra obtained on the 27 June, before size-resolved measurements were begun, and spectra from the 21 and 24 August, conducted before and after the measurement period, revealed similarities between the two months. From the ratio between CCN concentration and the total particle number concentration (CN) as a function of dry particle diameter (D_p) at a SS of 0.4%, the activation diameter (D_{50}), corresponding to CCN/CN = 0.50, was estimated. D_{50} was found to be 60 and 67 nm for the examined periods in June and August 2008, respectively. Corresponding D_{50} hygroscopicity parameter (κ) values were estimated to be 0.4 and 0.3 for June and August 2008, respectively. These values can be compared to hygroscopicity values estimated from bulk chemical composition, where κ was calculated to be 0.5 for both June and August 2008. While the agreement between the two months is reasonable, the difference

in κ between the different methods indicates a size-dependence in the particle composition, which is likely explained by a higher fraction of inorganics in the bulk aerosol samples.

1 Introduction

The Arctic represents a region of special interest for atmospheric research because it is: i) very sensitive to changes in radiative forcing owing to a direct feedback mechanism; ii) expecting greater anthropogenic activity from increased shipping and natural resource explorations in the near future and iii) yet poorly understood in terms of climate controlling processes, largely due to the lack of observational data. One of the most significant uncertainties in climate prediction is the role of clouds, and in particular, the influence of anthropogenic activities on clouds. In general, clouds have the ability to both cool the surface by reflecting incoming solar radiation back to space, or warm the surface by re-emitting long-wave radiation back to the surface (Boucher et al., 2013). The formation of clouds is dependent on the presence of excess water vapour in the air and on the presence of aerosol particles having cloud condensation nuclei (CCN) properties. Such particles must have sufficient size and hygroscopicity to act as sites for cloud droplet formation. In this study, two short case studies are presented, based on observations conducted in June and August 2008 at the Zeppelin station, Svalbard. These data complement the existing CCN and aerosol measurements conducted in the Arctic, but for the first time the CCN properties here are determined on-line as a function of dry particle size. Moore et al. (2011a) have provided a brief literature review of CCN measurements in the Arctic; however, to set our study in the context of other studies and to summarize the available information concerning Arctic CCN, we also present a short literature overview, including some of the most recent studies. For clarity, data are first grouped into land-based measurements, then measurements from ships and followed by aircraft measurements.

Land-based measurements

Shaw (1986) examined the CCN spectra of air masses characterized by Arctic haze during January and February 1985 in central Alaska. The maximum supersaturation (SS) was found to be around 0.33%, and the dominant CCN consisted of soluble particles at a concentration of a few hundred per cm^{-3}, characterized by a rather large size of approximately 1 μm.

Silvergren et al. (2014) presented chemical and physical properties of aerosols collected at the Zeppelin research station, Svalbard from September 2007 to August 2008. Hygroscopic growth and cloud forming potential were examined on a monthly basis. From this, it was shown that during the summer months, the SS has the greatest impact on the number of CCN. As the aerosol sulphate and nitrate mass concentrations reached a maximum between March and May, it was concluded that these months presented the most unfavourable cloud forming properties of the entire year. From September to February, sea salt was present in the highest mass concentrations. Both the growth factor and the values of the hygroscopicity parameter κ ranging approx. between 0.7 and 1 were determined to be highest in October, which was noted as the month with the most favourable cloud forming potential.

Ship-based measurements

Bigg & Leck (2001) reported the results from CCN measurements conducted on an icebreaker at latitudes higher than 80°N, from 15 July to 23 September 1996. They observed CCN concentrations between 1 and 1000 cm^{-3} at a SS of 0.25% over the measurement period. Daily median CCN concentrations at the same SS were around 15–50 cm^{-3}, and over the course of a day, concentrations could vary by up to one order of magnitude. A decrease in CCN concentration of approximately one order of magnitude was observed when air was being transported from the open ocean to the pack ice. The authors suggested that this occurred as a result of wet scavenging. However, after this 36 h-period, an increase in CCN concentration was observed, which was thought to be related to local aerosol production from bubble bursting occurring between the pack ice.

The results of CCN measurements conducted during three weeks in August and September 2008 on board the icebreaker 'Oden', which was drifting passively to the north of 87°N, are presented by Martin et al. (2011). A mean SS of 0.10% resulted in a mean CCN concentration of 14 ± 11 cm^{-3}, which increased up to 47 ± 37 cm^{-3} for a mean SS of 0.73%. In general, CCN closure within the measurement uncertainties was successful for SSs of 0.10%, 0.15% and 0.20%, assuming an internally mixed aerosol with a nearly insoluble organic volume fraction. However, the calculated CCN concentrations for SSs of 0.41% and 0.73% overestimated the measured CCN concentrations; this is suggested to be a result of differing chemical properties of different aerosol sizes.

Aircraft measurements

Hoppel et al. (1973) present results of aircraft measurements from February 1972 above Alaska, approximately 160 km north of Fairbanks. A strong temperature inversion was observed during the measurements, and an increase in CCN concentration, approximately from 100 to 400 cm^{-3}, was recorded to accompany an altitude increase, from 1.75 km to 4 km. Moreover, the increase of CCN concentration with an increase in SS was dependent on the altitude of the measurements. At 4.3 km altitude, the CCN concentration increased approximately from 50 cm^{-3} at 0.3% SS to 600 cm^{-3} at 1% SS. In contrast, at approximately 0.3 km above sea level, an increase of CCN concentration was observed approximately from 60 cm^{-3} at 0.3% SS to 100 cm^{-3} at 0.8% SS, but no further increase was seen up to a SS of 1%. Hoppel et al. (1973) suggested that these data may indicate the production of CCN in the upper troposphere or in the stratosphere, followed by downward mixing into the lower atmospheric layers.

CCN data from aircraft measurements conducted during April 1992 over the Arctic Ocean were presented by Hegg et al. (1995). Measurements took place around 350 km from the Alaskan coast between 0.03- and 4-km altitude; they show CCN concentration to vary between 19.9 and 92.7 cm^{-3}, with a mean value of 47 ± 19 cm^{-3} measured at 1% SS. Hegg et al. (1995) also observed an increase in CCN concentration with altitude up to 3 km, but note that the data points above 3-km altitude are too sparse to reliably predict any trend. Below 1.6-km altitude the fraction of particles that act as CCN ranged between 0.002 and 0.38 with an average of 0.15 ± 0.08 at 1% SS. No reliable CN data were obtained for altitudes higher than 1.6-km due to a frozen valve. Hegg et al. (1995) concluded that their data are an indication of particle production at higher altitudes compared to lower altitudes.

Results of aircraft measurements made during 11 flights over Alaska in June 1995 were published by Hegg et al. (1996) and compared to measurements presented in Hegg et al. (1995). This further study concluded that the fraction of activated particles is, on average, approximately 0.10 at a SS of 1%. They therefore suggested that the number of smaller particles is higher during June 1995 than in the spring of 1992.

Yum & Hudson (2001) presented vertical CCN profiles obtained at least 500 km north of the Alaskan coast during a flight campaign in May 1998. They observed a clear increase in CCN

concentration with an increase in altitude when low stratus clouds were present. However, under non-cloudy conditions, an increase in CCN concentration was only observed at heights with an air pressure lower than 700 mbar. Average CCN concentrations measured at a SS of 0.8% were 257 ± 79 and 76 ± 29 cm^{-3} above and below the stratus cloud, respectively. In contrast, the average CCN concentrations obtained at lower altitudes (comparable to the measurements beneath the clouds) during non-cloudy flights was 250 ± 41 cm^{-3}. The authors proposed that the CCN concentrations in the low cloudy boundary layer are controlled by cloud scavenging, resulting in a clearly altitude-dependent CCN density profile. Analyses of CCN spectra were also conducted, using the formula $N = C*SS^k$, where N is the CCN concentration at a given SS, C is the CCN concentration at 1% SS and k describes the slope of the function. The CCN spectra at specific height levels showed larger k values under the non-cloudy conditions, compared to when clouds were present (for example, 2.214 compared with 1.474 at 0.04%–0.1% SS and at 560–660 hPa), with the exception of the highest SS values found at lower altitudes.

Moore et al. (2011a) presented results from five research flights over the Alaskan Arctic during April 2008, beginning from Fairbanks and covering parts of the Beaufort Sea. The air masses sampled variously represented background conditions, biomass burning plumes, anthropogenic pollution and Arctic boundary layer conditions. Calculated activation curves with SS values ranging between 0.1% and 0.6% showed that at least 70% of the particles were activated for SS at around 0.2% for all air masses. It was therefore concluded that this similarity in observed activation pattern, despite the differences in chemical composition, is a result of aerosol size, which largely determines CCN activity. However, the authors pointed out that for SS between 0.3% and 0.6% it is likely that the particle chemical composition controls the maximum fraction of particles that can act as CCN.

Lathem et al. (2013) presented results of CCN measurements conducted during research flights from 26 June to 14 July 2008. The flight campaigns set-off from Cold Lake, Alberta, Canada and passed through the northeastern Canadian Arctic before heading to the west coast of Greenland. During the flights, the various air masses were characterized by biomass burning, boreal forest background, Arctic background and anthropogenic industrial pollution. Median CCN concentrations were highest for air masses influenced by fresh biomass burning, at 7778 cm^{-3} at standard temperature and pressure (STP, 1013 hPa and 273.15 K). At a SS of 0.55% the CCN/CN ratio was around 0.89 for those particles resulting from fresh biomass

burning. The lowest CCN/CN activation ratio was 0.15 at SS 0.55%, observed for air masses characterized by industrial pollution, with a CCN concentration of 341 cm^{-3}. The Arctic background air mass resulted in a moderate activation ratio of 0.52 for 0.5% SS, while CCN concentration was 247 cm^{-3}.

During a flight campaign over the northern slopes of Alaska in April 2008, Hiranuma et al. (2013) collected ambient particles, dry residuals of mixed-phase cloud droplets and ice crystals. They analysed their size and chemical structure using an electron microscope in combination with various X-ray techniques. Note that the results should be interpreted with caution due to the limited number of samples. However, the limited data showed that the residuals of cloud droplets were enriched with respect to carbonate and black carbon, compared to the ambient particles. Significant mixing was also observed in the cloud droplet residuals. Additionally, during a period of high ice nucleation efficiency, residuals were enriched in sodium and magnesium salts compared to the ambient particles.

The studies described above reveal the significant variability in CCN concentration across the Arctic, likely resulting from differing locations of CCN production (upper troposphere vs. lower boundary layer), production mechanisms, in-cloud processing and the origins of air masses. Several studies indicate an increase in CCN with increasing altitude in the lower half of the troposphere. However, the controlling mechanism for this increase is still unclear. In this study, we compare bulk CCN properties with those found in previous studies, and we also explore the size-dependence of CCN activation potential for the Arctic aerosols by combining a DMPS (Differential Mobility Particle Sizer) system with a CCN counter (CCNC). Although size dependent CCN activation has been studied worldwide (Bhattu & Tripathi, 2014; Rose et al., 2010; Paramonov et al., 2013; Gunthe et al., 2009), according to our knowledge, this is the first study presenting size-resolved CCN activation in the Arctic.

2 Methods

2.1 Location

Measurements were made at the Zeppelin research station (78°54'N, 11°53'E, 474 m above sea level), which is situated approximately 2 km south-west of the small settlement Ny-Ålesund, in Svalbard. The station is seldom affected by local pollution and therefore can be considered to represent remote Arctic atmospheric conditions. Continuous aerosol

measurements were begun in the year 2000, concerning which detailed information can be found in Tunved et al. (2013).

2.2 Instrumentation and experimental setup

Particle number size distributions were measured using a closed-loop Differential Mobility Particle Sizer (DMPS), consisting of a medium-sized Hauke Differential Mobility Analyzer (DMA) in combination with a TSI Condensation Particle Counter (CPC) 3010. Measurements were performed within 40 different size bins, with particle diameters ranging between 10 and 900 nm. Each particle size range was measured for 10 sec, followed by a lag time of 5 sec before the next size range was measured. Simultaneously, total particle number concentrations were precisely measured using a TSI CPC 3025 with a lower cut-off size of 3 nm, and by a TSI CPC 3010 with a lower cut-off size of 10 nm. A commercially available DMT CCN counter connected to a 1/4" stainless steel tubing inlet registered CCN concentrations at SSs of 0.2, 0.4, 0.6, 0.8 or 1 %."In the CCNC scanning mode, each SS level was measured for approximately 5 min before changing to the next SS level. After completing the 1% SS level, the measurements began again at 0.2% SS after at least a three min break in the measurements. The shared inlet of the DMPS, TSI CPC 3025, and TSI CPC 3010 was precipitation protected with an estimated cut-off size of 5 µm.

In the standard configuration these two instrument systems operate independently. In this study, however, we combined the two systems such that the DMA first selects a nearly mono-disperse aerosol, which is then supplied to the CCNC. For the CCN size-resolved concentration measurements, the CCNC was connected to the DMA and SS was fixed at 0.4%. The number of size bins of the DMPS system was also reduced from 40 to 15, and the time each particle size was measured was extended from 10 to 35 sec to improve counting statistics. The lower and upper bounds of the DMPS scans were also narrowed to 15 and 400 nm, respectively. The two different setups of the CCNC are shown in Fig. 1.

2.3 Experiments

Two case studies are presented here, consisting of CCN size-resolved number concentration measurements conducted during summer 2008. The measurement period for the first case study lasted from around 9:40 on 27 June to around 10:15 on 29 June during which about 290 size-resolved CCN scans were conducted. The minimum and maximum temperatures for this

period were 3.8 and 9.4°C, respectively. The measurement period for the second case study began at around 7:30 on 21 August and ended at around 10:50 on 24 August, resulting in about 374 size-resolved CCN scans. The minimum and maximum temperatures for this period were 2.8 and 5.9°C, respectively. Before the size-resolved CCN concentration measurements were performed in June, CCN spectra were obtained from the total aerosols over a period of approximately 5 h. Unfortunately, no spectra were measured directly after the first CCN size-resolved experiment ended on 29 June. However, during the study in August, CCN spectra were determined for approximately 17 h on 21 August, before the CCN size-resolved experiment began, and for approximately 13 h on 24 August after the experiment ended. In addition, 5-day backward trajectories were calculated on an hourly basis, using the online web version of the NOAA HYSPLIT Model (Draxler & Rolph, 2014; Rolph, 2014), to analyse the origins of the air masses from which the observed results presented in the next section were derived.

3 Results and Discussion

3.1 Time series analysis

Particle number size distributions observed from 27 to 30 June 2008 are presented in Fig. 2a. The vertical purple lines in this figure indicate the beginning and the end point of the measurement period for the size-resolved CCN number concentration data. Based on the particle number size distribution, at least three characteristic periods can be distinguished: i) from midnight to approximately midday of 27 June, when particles with diameters of approximately 70 nm dominate the particle concentration; ii) from midnight to approximately midday of 28 June, when particle number concentrations are highest for particle diameters of approximately 20 nm and iii) from approximately midday on the 29 of June to the following midnight, when the concentration of particles with diameters approximately between 20 and 70 nm increased to more than 1000 cm^{-3} (cf. Fig. 2a). For the period 27 to 29 June, 5-day backward trajectories were calculated for each hour (shown above Fig.2a and below Fig 2b). Air masses arriving between 0:00 and 11:00 at Zeppelin station are characterized by both, air coming from a southerly direction and air having its residence time exclusively at the high Arctic. From 12:00 on the 27 of June until midnight of the 29 of June air masses reaching Zeppelin station have a clear central Arctic origin. In addition to the trajectory analyses, Lidar measurements from Ny-Ålesund, part of the Micro Pulse Lidar Network

(http://mplnet.gsfc.nasa.gov/, accessed 28 November 2013) were investigated for the presence of clouds or precipitation in the vicinity of the Zeppelin station. All times mentioned in these data refer to Coordinated Universal Time. Lidar measurements on the 27 of June 2008 in Ny-Ålesund showed only high clouds (altitude > 5 km), from approximately 9:00. Before 9:00, cloud-free conditions predominated at the measurement site. High clouds and cloud-free conditions alternated during 28 and 29 June 2008; therefore, Zeppelin station can be regarded as cloud-free during this time (cf. Fig. 3).

The time series of particle number size distribution (Fig. 2a) is accompanied by two time series of total aerosol number concentrations for particles having a lower cut-off size of 3 and 10 nm, respectively (Fig. 2b). Although particles smaller than 10 nm are unlikely to be CCN, the combination of the two CPC instruments permit detection of particles that are a result of recent new particle formation. The combination of 5-day backward trajectory analyses, Lidar measurements, particle number size distributions and total aerosol concentration time series gives a rounded picture of the conditions that prevailed during the experimental period.

The entire period from 27 to 30 June 2008 is characterized by a maximum of particle concentrations occurring at particle diameters below 100 nm. This is in line with the results of Tunved et al. (2013), who analysed long-term particle number size distributions at Zeppelin station during the years 2000–2010. In their study, the authors concluded that the Arctic summer aerosol number size distribution (June–August) is characterized by a dominance of particles with diameters less than the accumulation diameter. It is proposed that these aerosols are most likely formed within the Arctic itself. This explanation of local production agrees with our calculated trajectories (Fig. 2), which show transport almost only within the Arctic. In addition, the Lidar data from the period from 27 to 30 June 2008 does not indicate any cloud processing of the aerosols in the lower atmosphere boundary layer at the measurement site.

From midnight to approximately midday of 27 June, particles with diameters of approximately 70 nm dominate the particle concentration. The associated trajectory plot (Fig. 2) indicates that this pattern may result from a mixture of air masses, originating from the Norwegian Sea as well as from the Arctic Ocean.

During the early morning hours of 28 June 2008 a sharp increase in total particle number concentration is observed (Fig. 2b). The highest concentration of particle numbers is found for particles with dry diameters of less than 20nm (Fig. 2a), which points together with the

sharp increase in particle number concentration towards new particle formation during previous hours.The process of particle formation is not yet fully understood (Komppula et al., 2003; Yli-Juuti et al., 2011; Ortega et al., 2012), but sulphuric acid and organic compounds have been found to be the key components (Riipinen et al., 2007; Kuang et al., 2008; Sipilä et al. 2010; Kulmala et al., 2013). Most nucleation events take place during the daylight hours, which indicates the importance of photochemistry in the nucleation process. However, at some locations particle formation events are also observed at night when there is no ambient light (Ortega et al., 2012). In Ny-Ålesund, the polar day lasts from around 18 April to 23 August; therefore, the measurements made herein during June 2008 lie within this daylight period. Tunved et al. (2013) presented averaged diurnal particle number size distributions for June, based on observations made during 2000–2010, and found that the concentrations of particles with diameters less than 20nm predominantly begin to increase at around noon. Here presented data indicate, that an increase of particle concentration occured later in the day. In the Arctic environment, it has been suggested that dimethyl sulphide plays an important role as a condensing vapour for the nucleation process (Chang et al., 2011). Tunved et al. (2013) stated that another requirement of particle nucleation in the Arctic is a low condensation sink, which means a low concentration of particles in the accumulation mode. These authors showed that the particle mass is strongly related to accumulated precipitation along the transport path (cf. Figure 15 in Tunved et al., 2013), and that conditions are favourable for new particle formation during the period of midnight sun. Integrated precipitation over the five day duration was calculated for each hourly trajectory. Over all there was little precipitation during the investigated periods with a median of less than 3.7 mm for the June case and less than 1.7 mm for the August case. The maximum integrated precipitation is an isolated event for a trajectory arriving 0600 on 27 June. For this trajectory the integrated precipitation was 18.5 mm. From this we can conclude that recent precipitation within the last five days was not likely a dominant factor in shaping the aerosol properties during transport.

From midday on 29 June 2008 until approximately 22:30 on that day, the total particle number concentrations of particles with diameters greater than 3 nm increased approximately from 400 cm^{-3} to 3860 cm^{-3} (Fig. 2b). The highest concentrations were found for particles with diameters between 30 and 70 nm. A change in the height pattern of the trajectories is seen between the midday of the 29 June and the following hours (Fig. 2). It seems that the air masses´ height is reduced and it is possible that this change in transport pattern resulted in

more moisture supply to the air mass which helped promote particle formation and growth when the sun was at its highest.

To place the period in which the size-resolved CCN measurements were conducted in a long-term context, the median of the total particle number concentration for particles with diameters greater than 10 nm during this period is compared with the medians of the June data for the years 2001–2010 (Tunved et al., 2013). The long-term data have a time resolution of 1 h, but around 9% of these data are missing or are of poor quality and are therefore not considered in the calculation. The data are available within specific size distributions, and the total number was calculated by integrating over the distinct size ranges. From 2001 to 2005 the lowest measured size was 17.8 and the largest was 707.9 nm. From 2006 to 2007 a size bin with a lower measurement range of 13.8 nm was added. For 2008–2010 the size distribution diameter range was again broadened, to range between 10 and 790 nm. The calculations resulted in a median particle number concentration of 177 cm^{-3} for 2001–2010, with a 25^{th} percentile of 80 cm^{-3} and a 75^{th} percentile of 339 cm^{-3}. The median values with 25^{th} percentile and 75^{th} percentile for the period during which our CCN size-resolved measurements were conducted during June 2008 are 245, 195 and 292 cm^{-3}, respectively. Although the median total particle number concentration is somewhat 40% higher than the averaged June data from 2001 to 2010, it falls within the 75^{th} percentile of the long term data. This in combination with the low particle concentrations in the accumulation mode and the occurrence of a nucleation event indicates that the case study data from June 2008 can be regarded as relatively representative.

Particle number size distributions from 21 to 25 August 2008 are presented in Fig. 4a. In this figure, the purple vertical lines indicate the start and end times for the CCN size-resolved concentration measurements. Difficulties with the DMPS measurements occurred approximately from 8:00 to 19:30 on 21 August and for short periods on 22 August; these time periods are omitted from the analysis. The particle number size distribution time series represent time series of total particle number concentrations with dry diameters greater than 3 and 10 nm, respectively (cf. Fig. 4b). As with the measurements from June 2008, different periods with different characteristic particle number size distributions can be distinguished during the studied time period in August 2008 (Fig. 4a): i) the final hours of 21 August, when particle number concentrations were highest for particles with diameters between 100 and 200 nm; ii) the early morning hours of 23 August, when particle number concentrations were

relatively low for all measured sizes (cf. Fig. 4b) and iii) during the first half of 24 August, when total aerosol concentrations were relatively high for the period, but no particular size range clearly dominated. Calculated 5-day backward trajectories for each hour indicate that air masses arriving on the 21 August at Zeppelin station mainly come from the southern part of the Norwegian Sea (Fig. 4). Air masses arriving from the 22 August until midday the 24 August at Zeppelin station have a more northern origin, the Barents Sea Air masses arriving between midday and midnight on the 24 of August at Zeppelin station have again an origin over the Norwegian Sea.

As with the measurement period in June 2008, Lidar data were consulted to investigate any local effects from clouds and precipitation (cf. Fig. 5). During the 21 August 2008, apparently clouds are present approximately between 0.7 and 9 km above the Zeppelin station. However, no precipitation reaching the station level could be detected. On 22 August low clouds (altitude < 2 km) were observed from approximately 9:00, and precipitation started at approximately 24:00, continuing until approximately 9:00. Only a few precipitation events are observed on 23 August 2008 for the most part, no clouds are observed at the altitudes above the Zeppelin station. On 24 August, clouds were only observed in Ny-Ålesund at altitudes higher than 0.8 km.

From around 20:00 to 23:00 on 21 August 2008, particles with dry diameters between 100 and 200 nm dominate the particle number size distribution. During the time period of 2:00 and 24:00 on the 21 of August, the Zeppelin research station was according to the Lidar measurements very likely unaffected by clouds. The trajectories of the 21 August show that air masses originate from the mid-latitudes and lower their height when reaching Zeppelin research station (Fig. 4). Therefore, it is likely that the peak in the particle number size distribution for particles with diameters between 100 nm and 200 nm is a result of particles being transported from the mid-latitudes to the Arctic and the processes taking place during transport rather than particles are being produced locally. The accumulation mode-dominated size distribution differs somewhat from the typical summer conditions. Tunved et al. (2013) demonstrated from their long-term average, during June–August, which locally produced particles with diameters in the nucleation and Aitken mode dominate the particle number size distribution. In the morning hours of 23 August 2008, air masses arriving at Zeppelin station originated in the Barents Sea (Fig. 4) and resulted in relatively low total particle concentrations, compared to the concentrations observed between 20:00 and 23:00 on 21

August 2008 (Fig. 2b). Air masses in the morning of the 24 of August originated as well in the Barents Sea, but result in higher total particle concentrations than observed on the 23 of August.

To place our second case study data in a long-term context, we compare median values of August 2008 with the 10-year climatology presented by Tunved et al. (2013). Approximately 12% of the hourly data were excluded from calculations of the median integrated particle number concentration from 2001 to 2010 August, owing to them being either missing or of poor quality. The calculations produced a median particle number concentration of 127 cm^{-3} for August during 2001–2010, with a 25^{th} percentile of 58 cm^{-3} and a 75^{th} percentile of 252 cm^{-3}. In comparison, the median values with 25^{th} percentile and 75^{th} percentile for the size-resolved CCN measurement period in August 2008 are 226, 147 and 329 cm^{-3}, respectively. Although, the total particle number concentration during the period in which the CCN size-resolved measurements were conducted is about 80 % higher than the long-term average, the particle number concentration still falls within the 75^{th} percentile.

Overall, the June case is similar to the long-term climatology and appears to be more representative of the summer period, with air masses of Arctic origin. In contrast, the August case differs more from the long-term climatology and shows a more significant influence of lower latitudes and higher number densities of accumulation particles.

3.2 CCN spectra

A CCN spectrum for a 5 h-long period on the 27 June 2008 was obtained before the size-resolved CCN measurements were begun. The data presented in this section comprise medians calculated from one SS scanning cycle. The ratio, as function of SS, between CCN number concentration and the total particle number concentrations for particles with diameters greater than 3 nm ($CN_{>3nm}$) for 27 June 2008 is shown in Fig. 6a. A significant increase in the ratio of CCN to CN with an increase in SS is detectable by applying the two-sample Kolmogorov–Smirnov test, only for an increase in SS from 0.2% to 0.4%. The absolute number of CCN dependent on SS is shown for 27 June 2008 in Fig. 6b. Applying the two-sample Kolmogorov–Smirnov test to the data resulted in a significant difference in CCN numbers with increasing SS (5% significance level). The power-law function, $N_{CCN}(SS) = C*SS^k$, describing the number of CCN (N_{CCN}) with the coefficients C and k and SS, was fitted to the data shown in Fig. 6b and giving values for the coefficients of C = 221 and k = 0.482.

Ranges in the parameters C and k depend on the type of air mass, and the values for 27 June 2008 will be discussed in a later section, in combination with the values obtained from the August 2008 data.

CCN spectra obtained during 17 h and 13 h observation periods on 21 and 24 August 2008, respectively, are shown on the right side of Fig. 6. The ratios between CCN and CN as a function of SS are shown in Fig. 6c for the two different days. For 21 August, a significant increase in the CCN to CN ratio with an increase in SS was observed in all cases. For 24 August, the increase in ratio was significant for all increases in SS, except for the increase from 0.4% to 0.6% SS. The absolute number of CCN for 21 and 24 August, as a function of SS, is shown in Fig. 6d. For both days, the increase in CCN number from one SS to the next is significant. This is based on applying the two-sample Kolmogorov–Smirnov test with a 5% significance level. As with the same data from 27 June 2008 (cf. Fig. 6b), a power-law function of the same form was fitted to the data from 21 and 24 August 2008, as denoted by the red lines in Fig. 6d. The fittings resulted in C = 251 and C = 146 and k = 0.367 and k = 0.446 for 21 and 24 August 2008, respectively.

Rogers & Yau (1996) demonstrated that the coefficients for maritime air vary, with C = 30–300 cm^{-3} and k = 0.3–1.0, while for continental air the values vary between C = 300–3000 cm^{-3} and k = 0.2–2.0. The coefficients C and k that are given by the fitted power-law function applied to the measurements during June and August 2008 (cf. Fig 6b and Fig. 6d) are consistent with the ranges that Rogers & Yau (1996) proposed for maritime air masses. Pruppacher & Klett (2010) also presented a compilation of C and k values from different studies, alongside the CCN/CN ratio for a SS of 1% at different locations, characterized by either maritime or continental air masses. Only one study from the Arctic, influenced by a maritime air mass, is presented, providing a C value between 100 and 1000 cm^{-3}. Pruppacher & Klett (2010) did not present a k value for this study, but stated that the CCN/CN at 1% SS is 0.5. Compared to the data from Zeppelin in this study, this range is at the lower limit of that observed on 21st August 2008, and at the upper limit of that observed on 27 June and 24 August 2008 (cf. Fig. 6a and Fig. 6c). However, it should be noted that direct comparison is difficult as it is not known which size range was considered for the integrated number of CN. Hegg et al. (1995) also presented a number of C and k values and CCN/CN ratios obtained during several flight campaigns over the Arctic. Although an increase in CCN was observed with an increase in altitude for a SS of 1%, CCN concentrations for altitudes < 1.6 km were

always lower than 100 cm^{-3}. This is in contrast to the measurements obtained at Zeppelin station in this study, where CCN concentrations were generally higher than 100 cm^{-3} at a SS of 1% (cf. Fig. 6b and Fig. 6c). The average CCN/CN ratio for measurements conducted at altitudes lower than 1.6 km was calculated to be 0.15 (Hegg et al., 1995), which is lower than the calculated average ratios of 0.32, 0.77 and 0.38 obtained for a SS of 1% for 27 June, 21 and 24 August 2008.

Yum & Hudson (2001) estimated an average CCN concentration of 76 cm^{-3} in conditions when low clouds are present and an average of 250 cm^{-3} for non-cloudy conditions at a SS of 0.8%. Estimating the CCN concentration at 0.8% SS with the power-law function results in CCN concentrations of 199 cm^{-3}, 231 and 132 cm^{-3} for 27 June, 21 and 24 August, respectively. For 27 June only high clouds (altitude > 5 km) were present, while for 21 and 24 August clouds were observed at altitudes higher than 0.7 km (cf. Sect. 3.1). The CCN concentrations calculated herein using the power law relation and a SS of 0.8% for June and August clearly lies between those CCN concentrations determined by Yum & Hudson (2001) for non-cloudy conditions. The CCN/CN ratio calculated by Yum & Hudson (2001) is 0.65 at a SS of 0.8%, which is higher than the average ratio determined for the CCN spectra during 27 June and 24 August 2008. The arithmetic means of the CCN/CN ratio at a SS of 0.8% are 0.31, 0.75 and 0.35 for 27 June, 21 and 24 August 2008, respectively. Yum & Hudson (2001) also present altitude-dependent k values for a SS range of 0.1%–0.6%. The k values for cloudy conditions ranged between 0.27 and 0.55 and between 0.34 and 0.75 for non-cloudy conditions. Calculated k values for 27 June, 21 and 24 August 2008, only considering a SS range of 0.2% to 0.6%, were found to be 0.65, 0.41 and 0.37, which is similar to the results obtained by Yum & Hudson (2001).

Silvergren et al. (2014) presented CCN number concentrations as a function of SS and as a function of the month from September 2007 to August 2008, calculated based on aerosol collections on filters at Zeppelin research station. For June 2008, a CCN number concentration of around 100 cm^{-3} at a SS of 0.4% is shown. This concentration is lower than the calculated CCN number concentration found here using the power-law relation shown in Fig. 6 and a SS of 0.4%, which results in a CCN number concentration of 142 cm^{-3}. For August 2008, Silvergren et al. (2014) calculated a CCN number concentration of approximately 65 cm^{-3} at 0.4 % SS for the Zeppelin research station, which is although lower

than the concentrations of 179 and 97 particles cm^{-3} calculated from the presented data in Fig. 6d for 21 and 24 August 2008.

No clear separation can be made between the two CCN spectra from August 2008 and the one CCN spectrum from June 2008. In general, the CCN spectrum of June 2008 (Fig. 6b) lies between the two different spectra of August 2008 (Fig. 6d). Comparing backward trajectories arriving at Zeppelin before midday the 27 June (Fig. 2) and before midday the 21 August and after midday the 24 August (Fig. 4), corresponding to the times when the CCN spectra were measured, show that the air masses' origin was for the most of the times southerly of Svalbard. However, even those air masses with similar origins can show differences in their aerosol characteristics (Park et al., 2014).

3.3 CCN activation diameter

The size-resolved activation of particles having D_p between 15 and 400 nm at 0.4% SS is shown in Fig. 7. The upper panel shows the geometric mean of the activated particle concentration measured by the CCNC compared to the geometric mean of the total particle (CN) concentration measured by the CPC for the measurement period during June 2008 (Fig.7a). The lower panel shows the correspondent data for the measurement period in August 2008 (Fig. 7b). The most distinct differences between the particle number concentrations of total particles measured by the CPC during the experimental period in June 2008 and August 2008 is a) a higher particle number concentration having $D_p < 20$ nm during June; b) a peak of particle concentration at approximately D_p 50 nm in August and c) a higher variation in particle concentration for the different size bins indicated by a higher geometric SD during August compared to June. As the CN number concentration, the CCN concentration is characterized by a higher variability during the measurement period in August compared to the measurement period in June.

To establish the presented study contextually with other studies, the ratio between CCN and CN as a function of dry particle diameter was calculated (Fig. 8). Note that during June the CCN concentration exceeds the total particle concentration for $D_p > 156$ nm, and during August the CCN concentration is higher than the CN concentration for $D_p < 19$ nm and $D_p > 123$ nm. The experimental approach of selecting a narrow size range that can be applied to the CCNC results in very low particle concentrations in the instrument. In particular, for measurements made at either end of the size distribution, small errors can cause large changes

in the ratio, as presented in Fig. 8. To obtain completeness, all data points are shown; however, the sizes where CCN/CN ≥ 1 have been shaded and disregarded.

After applying a spline interpolation to the measurement data, the dry diameter at which 50% of the total particle number concentration was activated (D_{50}) was calculated to be 60 nm for the measurement period in June 2008 and 67 nm in August 2008. To the best of our knowledge, to date no size-resolved CCN measurements in the Arctic have been published; therefore, data are compared to results obtained in the subarctic. Anttila et al. (2012) reported a study that was conducted at the Finnish Pallas-Sodankylä Global Atmospheric Watch station that measured the ratio between cloud droplet number concentration and total particle concentration while the station was in clouds as a function of dry particle size. By comparing CCN concentrations at a fixed SS of 0.4% with cloud droplet number concentrations, it was concluded that during the cloud events the "effective" maximal SS was likely to be approximately 0.4% in most cases. During the five periods when the station was in clouds, D_{50} varied between 80 and 102 nm on average. A comparable study at the same measurement site resulted in D_{50} between 110 and 140 nm for maximal SS between 0.18% and 0.26% (Anttila et al., 2009). Komppula et al. (2005) calculated D_{50} by comparing a particle number size distribution measured at a site in clouds with a nearby measured size distribution obtained at a station under cloud-free conditions. D_{50} was estimated to be 80 nm on average and varied between 50 and 128 nm. Unfortunately, the SS is unknown. Due to the uncertainty in SS, it is not possible to compare present study to the studies conducted at the Finnish stations directly. However, due to SS lower than 0.4% reported by Anttila et al. (2012) and Anttila et al. (2009), larger activation diameters in these studies compared to this study are expected, which is in line with the presented results. Jaatinen et al. (2014) report activation diameters for measurements conducted during the same field campaign as reported in Anttila et al. (2012). However, compared with Anttila et al. (2012), in the present study, activation diameters were calculated differently and for a shorter period. The critical diameter was calculated by interpolating between the size bin at which the integrated particle number size distribution was equal to the amount of total measured CCN and the previous size bin. This resulted in a critical diameter of 98±16 nm for 0.4% SS (Jaatinen et al., 2014).

Besides SS, the chemical composition and mixing state determines the ability of particles to become activated to cloud droplets (Frosch et al. 2011; Moore et al., 2011b; Ervens et al., 2010; Sullivan et al., 2009). Kreidenweis et al. (2005) summarize results of predicted and

experimentally determined critical diameters of ammonium sulphate and sodium chloride particles. Predicted critical diameters for sodium chloride particles vary between 44.6 and 39.4 nm (Kreidenweis et al., 2005 and references therein) and the experimentally determined diameter for a SS of 0.4% was reported to be 40±6 nm (Corrigan & Novakov, 1999 in Kreidenweis et al. 2005). Ammonium sulphate particles had larger predicted activation diameters at SS of 0.4%, i.e., from 62.6 to 49 nm (Kreidenweis et al., 2005 and references therein). Experimentally determined critical diameters of ammonium sulphate were 51 ± 8 and 59 ± 9 nm (Corrigan & Novakov, 1999 and Kumar et al., 2003 in Kreidenweis et al., 2005). Corrigan and Novakov (1999) experimentally estimated D_{50} measured at a SS of 0.4% to be 82 nm, 148 and 74 nm for succinic acid, adipic acid and glucose aerosols, respectively. It was concluded that all D_{50} match well with the D_{50} calculated theoretically, except for the less soluble adipic acid. Kumar et al. (2003) experimentally determined the activation diameter of oxalic acid to be 65 nm at a SS of 0.40%. In the following section, the obtained information of the activation diameter, as well as the chemical information about the aerosol at the Zeppelin research station from another study are used to calculate the hygroscopicity parameter κ.

3.4 Comparison of κ values obtained with different methods

The hygroscopicity parameter κ was first introduced by Petters and Kreidenweis (2007) to describe the relationship between particle dry diameter and CCN activity. In this study, κ values were calculated with two independent approaches for June and August 2008: 1) based on the CCN activation of the aerosol population; 2) based on the bulk chemical composition of the particulate mass sampled at the site.

First, the relationship between the activation diameter ($D_{p,act}$) and *SS* derived from κ-Köhler theory (Asa-Awuku et al., 2010) was applied to the experimental CCN data:

$$SS = \frac{2}{3}\left[\frac{4M_w\sigma}{RT\rho}\right]^{3/2}\left(3\kappa D_{p,act}^3\right)^{-1/2}. \quad (1)$$

where M_w (kg mol^{-1}) is the molar mass of water, T is the temperature, R is the universal molar gas constant, σ is the surface tension of the solution/air interface and ρ (kg m^{-3}) is the density of the solution. The surface tension of pure water 0.072 J m^2 and the density of pure water 1000 kgm^{-3} were applied. Temperature was assumed to be 295 K to match the temperature in the instruments. When analysing the experimental data, the activation diameter was assumed

to be the dry diameter corresponding to the CCN to CN ratio of 0.5. However, we tested the sensitivity to this assumption by repeating the calculations for CCN/CN values of 0.25 and 0.75. The resulting κ values were 0.2–0.7 for June and 0.2–0.5 for August, with the best estimates (corresponding to the 50%-points in the CCN/CN ratios) of 0.4 and 0.3, respectively (Table 1).

Second, the κ values derived from the CCN activation data were compared to κ values obtained using the aerosol composition data. In this case, the total κ for the multi-component aerosol particles was calculated using the simple mixing rule

$$\kappa = \sum_i \varepsilon_i \kappa_i \cdot \qquad (2)$$

where ε_i and κ_i are the volume fraction and hygroscopicity parameter of each component i, respectively (Petters & Kreidenweis, 2007). We assumed internally mixed aerosol particles, composed of four surrogate components (inorganics, more water-soluble organics, less water-soluble organics and elemental carbon, similar to Rastak et al., 2014; see Table 2 for the assumed single-component properties). The monthly mass fractions of the organic components were estimated by analysing filter samples of particles that passed a PM_{10} inlet. The inorganic fraction was determined after sampling the aerosol with an open face system without a PM_{10} inlet but shielded with a cylinder that reduced the sampling efficiency for particles larger than 10 μm (Silvergren et al., 2014). It should be noted that the properties of ammonium sulphate were used to describe the inorganic fraction. The sea salt contribution in the inorganic fraction was not considered for particles less than 400 nm (upper bound of the DMPS in this study). The resulting total κ values were approximately 0.5 for both considered months (Table 2).

Comparison of the "bulk κ" (obtained with Eq. (2) and bulk chemical composition) with the "CCN κ" (obtained from the CCN/CN = 0.50 point with Eq. (1)) shows reasonable agreement for June but a slight overestimation for August. This could be due to the overestimation of the inorganic fraction in the "bulk κ", as particles with diameters >400 nm were also able to reach the filter. The chemical composition was therefore probably not accurately representative of the CCN-sized particles. In addition, it should be noted that the data used to calculate κ with Eq. (1) are based on only 2–3 days of measurements during June and August 2008 while the calculations used in Eq. (2) are based on bulk aerosol properties over the whole month of June and August 2008.

Silvergren et al. (2014) used three different approaches to calculate κ for June 2008 and August 2008. Bulk aerosol samples on filters were obtained during June and August 2008 at the Zeppelin research station. The filters were extracted and the extract was again filtered so that only the water-soluble fraction of the aerosols remained. With the first two approaches, particles were generated by an atomizer and then measured in a Hygroscopic Tandem Differential Mobility Analyser (HTDMA) and a CCNC. The corresponding κ values were calculated based on determined growth factors and critical SS and were estimated to be approximately between 0.4 and 0.5 on an average for both June and August 2008. In the third method, Silvergren et al. (2014) used the chemical information from the filter samples in combination with literature values to determine the activation diameter and the critical SS based on Köhler theory. The resulting κ values were approximately 0.7 for both June and August 2008 (cf. Fig. 9 in Silvergren et al., 2014). In present study, the "CCN κ" value for June was 0.4, which is in the lower end of results reported by Silvergren et al. (2014). For August, "CCN κ" was 0.3, which is lower than the results presented by Silvergren et al. (2014). The "bulk κ" values determined here are within the ranges determined by Silvergren et al. (2014) based on HTDMA and CCNC measurements.

Based on aerosol optical properties, Zieger et al. (2010) determined a mean κ value of 0.6 for the period July to October 2008 at the Zeppelin research station. The value presented by Zieger et al. (2010) is somewhat higher than the "bulk κ" estimated in this study (0.5 for both months). Conversely, the κ values calculated from the D_{50} using the DMPS-CCNC combination are clearly lower (0.4 for June, and 0.3 for August).

The main reason for the differences between the present study and both Zieger et al. (2010) and Silvergren et al. (2014) is probably related to the influence of large (>400 nm) particles in determining κ based on aerosol optical properties and the bulk chemical composition.

Anttila et al. (2012) reported a κ value of approximately 0.1 at Pallas for the same period as he presented activation diameters for (cf. Sect 3.3). The presented κ values are based on HTDMA measurements at 90% relative humidity for particles with D_d = 100 nm. Jaatinen et al. (2014) presented κ values obtained during the same measurement campaign as Anttila et al. (2012). However, the hygroscopicity parameter was determined differently and for a shorter period. The κ value derived by the critical diameter (cf. Sect 3.3) for a SS of 0.4% was estimated to be approximately 0.1 and thus is in agreement with the HTDMA-based observations of particles with D_d = 100 nm reported by Anttila et al. (2012). Conversely, the κ

calculated based on Aerosol Mass Spectrometer (AMS) data collected approximately 6 kilometres from the site of the CCN and HTDMA measurements was approximately 0.3. The "CCN κ" values determined in this study are higher than those obtained by Anttila et al. (2012) and Jaatinen et al. (2014). These differences can be explained by the different chemical composition of the aerosol population. Jaatinen et al. (2014) showed that at Pallas 47% of the measured mass concentration of the aerosols consisted of organic compounds, while at Zeppelin 90% of the aerosol mass was inorganic material and thus more hygroscopic material.

4 Summary and Conclusions

For the first time, size-resolved CCN measurements in the Arctic have been reported. Measurements were conducted at the Zeppelin research station, Svalbard during two short periods in June and August 2008. A near monodisperse aerosol having a D_p between 15 and 400 nm was selected by a DMA. The DMA was connected to a CCNC operating at 0.4% SS and in parallel to a CPC 3010. Before and after the size-resolved CCN measurements were taken, the CCNC was measuring the ambient air without previous selection of a monodisperse aerosol. During these periods, the SS in the CCNC was changed to 0.2%, 0.4%, 0.6%, 0.8% and 1%.

Trajectory analysis showed that during the measurement period in June 2008 air masses arriving at Zeppelin were dominated by Arctic air, while during August 2008 air masses originated from the Norwegian Sea and from the Barents Sea. A comparison of long-term June particle number size distributions with those registered during the size-resolved CCN measurements in June 2008 showed that the size distribution characterized by a nucleation event and low particle concentrations for $D_p < 100$ nm is representative for averaged conditions during June. In contrast, the particle number size distributions registered during August 2008 indicate long-range transport that differs from the long-term observations during August. In addition to the size-resolved CCN measurements, SS spectra were determined. In June, this was done directly before the size-resolved measurements were completed and in August directly before and after the size-resolved measurements were conducted. A power-law function of the form $N_{ccn}(SS) = C^* SS^k$, with N_{ccn} as the number of CCN and the coefficients C and k, was fitted to the SS spectra. The coefficients for June were estimated to be C = 221 and k = 0.482. Coefficients for August were C = 251 and k = 0.367 before the size-resolved measurements were conducted and C = 146 and k = 0.446 after the size-

resolved measurements were conducted. The spectra measured during June lies between the two measured during August. For a SS of 0.4%, CCN number concentrations as a function of dry particle diameter were presented. From the size dependent CCN measurements, D_{50} (particle diameter where CCN/CN = 0.5) was estimated. For the June 2008 measurement period, D_{50} was 60 nm, while for the August 2008 measurement period, D_{50} was approximately 67 nm. For the first time κ values for the Arctic were calculated based on activation diameters obtained from in-situ size-resolved CCN measurements, meaning the κ values are based on a conserved chemistry of the particles. Values of the hygroscopicity parameter κ were calculated to be 0.4 and 0.3 for June and August, respectively. Estimating κ based on simplified bulk chemical properties that were observed in June and August (2008) gave a value of 0.5. The higher κ value based on chemistry is likely explained by an enhanced influence of larger and more hygroscopic particles. It should be considered that, due to their lower numbers, these larger particles are less crucial for CCN activation. Therefore, the κ values based on in-situ measured size-resolved CCN measurements and growth factors are probably more meaningful in characterizing the ability of an aerosol population to become activated to cloud droplets. In future, it is needed to establish long term size-resolved CCN measurements in the Arctic to study the size dependent activation of particles for different seasons. An analysis of the difference in resulting κ values with κ values resulting from long-term chemistry analysis of the particles is needed to quantify and explain the reason for the differences and to point out possible differences to κ to the cloud model community.

Acknowledgements

We would like to thank Peter Tunved for providing the DMPS and CPC data. We acknowledge that the CCN measurements were supported by the KOPRI project NRF-2011-0021063. The authors gratefully acknowledge the NOAA Air Resources Laboratory (ARL) for the provision of the HYSPLIT transport and dispersion model and the READY website (http://www.ready.noaa.gov) used in this publication. The Swedish Environmental Protection Agency (NV) is acknowledged for their financial support of measurements at the Zeppelin station. We would like to point out that the NASA Micro-Pulse Lidar Network is funded by the NASA Earth Observing System and Radiation Sciences Program. We thank the MPLNET PI Masataka Shiobara and MPLNET staff Kerstin Binder for their efforts in establishing and

689 maintaining the Lidar measurements at Ny-Ålesund. The CRAICC project and the Bolin
690 Center for Climate Research are as well acknowledged.
691

692 References

693 Anttila T., Vaattovaara P., Komppula M., Hyvärinen A.-P., Lihavainen H., Kerminen V.-M.,
694 and Laaksonen A. (2009): Size-dependent activation of aerosols into cloud droplets at a
695 subarctic background site during the second Pallas Cloud Experiment (2nd PaCE): method
696 development and data evaluation, Atmos. Chem. Phys., 9, 4841-4854.

697 Anttila T., Brus D., Jaatinen A., Hyvärinen A.-P., Kivekäs N., Romakkaniemi S., Komppula
698 M., and Lihavainen H. (2012): Relationships between particles, cloud condensation nuclei
699 and cloud droplet activation during the third Pallas Cloud Experiment, Atmos. Chem. Phys.,
700 12, 11435-11450.

701 Asa- Awuku A., Nenes A., Gao S., Flagan R. C., and Seinfeld J. H. (2010): Water- soluble
702 SOA from Alkene ozonolysis: composition and droplet activation kinetics inferences from
703 analysis of CCN activity, Atmos. Chem. Phys., 10, 1585–1597.

704 Bhattu D. & Tripathi S. N. (2014): Inter-seasonal variability in size-resolved CCN properties
705 at Kanpur, India, Atmospheric Environment, 85, 161–168.

706 Bigg E. K. & Leck C. (2001): Cloud-active particles over the central Arctic Ocean, J.
707 Geophys. Res., 106(D23), 32155-32166.

708 Boucher O., Randall D., Artaxo P., Bretherton C., Feingold G., Forster P., Kerminen V.-M.,
709 Kondo Y., Liao H., Lohmann U., Rasch P., Satheesh S. K., Sherwood S., Stevens B., and
710 Zhang X. Y. (2013): Clouds and Aerosols. In: Climate Change 2013: The Physical Science
711 Basis. Contribution of Working Group I to the Fifth Assessment Report of the
712 Intergovernmental Panel on Climate Change [Stocker T.F., Qin D., Plattner G.-K., Tignor M.,
713 Allen S.K., Boschung J., Nauels A., Xia Y., Bex V. and Midgley P.M. (eds.)]. Cambridge
714 University Press, Cambridge, United Kingdom and New York, NY, USA

715 Chang R. Y.-W., Sjostedt S. J., Pierce J. R., Papakyriakou T. N., Scarratt M. G., Michaud S.,
716 Levasseur M., Leaitch W. R., and Abbatt J. P. D. (2011): Relating atmospheric and oceanic
717 DMS levels to particle nucleation events in the Canadian Arctic, J. Geophys. Res., 116,
718 D00S03.

719 Corrigan C. E. & Novakov T. (1999): Cloud condensation nucleus activity of organic
720 compounds: a laboratory study, Atmospheric Environment, 33, 2661-2668.

721 Draxler R. R. & Rolph G. D. (2014): HYSPLIT (HYbrid Single-Particle Lagrangian
722 Integrated Trajectory) Model access via NOAA ARL READY Website
723 (http://ready.arl.noaa.gov/HYSPLIT.php). NOAA Air Resources Laboratory, Silver Spring,
724 MD.

725 Ervens B., Cubison M. J., Andrews E., Feingold G., Ogren J. A., Jimenez J. L., Quinn P. K.,
726 Bates T. S., Wang J., Zhang Q., Coe H., Flynn M., and Allan J. D. (2010): CCN predictions
727 using simplified assumptions of organic aerosol composition and mixing state: a synthesis
728 from six different locations, Atmos. Chem. Phys., 10, 4795–4807.

729 Frosch M., Prisle N. L., Bilde M., Varga Z., and Kiss G. (2011): Joint effect of organic acids
730 and inorganic salts on cloud droplet activation, Atmos. Chem. Phys., 11, 3895–3911.

731 Gunthe S. S., King S. M., Rose D., Chen Q., Roldin P., Farmer D. K., Jimenez J. L., Artaxo
732 P., Andreae M. O., Martin S. T., and Pöschl U. (2009): Cloud condensation nuclei in pristine
733 tropical rainforest air of Amazonia: size-resolved measurements and modeling of atmospheric
734 aerosol composition and CCN activity, Atmos. Chem. Phys., 9, 7551-7575.

735 Hegg D. A., Ferek R. J., and Hobbs P. V. (1995): Cloud Condensation Nuclei over the Arctic
736 Ocean in Early Spring, J. Appl. Meteor., 34, 2076-2082.

737 Hegg D. A., Hobbs P. V., Gassó S., Nance J. D., and Rangno A. L. (1996): Aerosol
738 measurements in the Arctic relevant to direct and indirect radiative forcing, J. Geophys. Res.,
739 101(D18), 23349-23363.

740 Hiranuma N., Brooks S. D., Moffet R. C., Glen A., Laskin A., Gilles M. K., Liu P.,
741 Macdonald A. M., Strapp J. W., and McFarquhar G. M. (2013): Chemical characterization of
742 individual particles and residuals of cloud droplets and ice crystals collected on board
743 research aircraft in the ISDAC 2008 study, J. Geophys. Res. Atmos., 118, 6564-6579.

744 Hoppel W. A., Dinger J. E., and Ruskin R. E. (1973): Vertical Profiles of CCN at Various
745 Geographical Locations, J. Atmos. Sci., 30, 1410-1420.

746 Jaatinen A., Romakkaniemi S., Anttila T., Hyvärinen A.-P., Hao L.-Q., Kortelainen A.,
747 Miettinen P., Mikkonen S., Smith J. N., Virtanen A., and Laaksonen A. (2014): The third
748 Pallas Cloud Experiment: Consistency between the aerosol hygroscopic growth and CCN
749 activity, Boreal Env. Res. 19 (suppl. B), 368-382.

Komppula M., Lihavainen H., Hatakka J., Paatero J., Aalto P., Kulmala M., and Viisanen Y. (2003): Observations of new particle formation and size distributions at two different heights and surroundings in subarctic area in northern Finland, J. Geophys. Res., 108, 4295, D9.

Komppula M., Lihavainen H., Kerminen V.-M., Kulmala M., and Viisanen Y. (2005): Measurements of cloud droplet activation of aerosol particles at a clean subarctic background site, J. Geophys. Res., 110, D06204.

Kreidenweis S. M., Koehler K., DeMott P. J., Prenni A. J., Carrico C., and Ervens B. (2005): Water activity and activation diameters from hygroscopicity data–Part I: Theory and application to inorganic salts, Atmos. Chem. Phys., 5, 1357-1370.

Kuang C., McMurry P. H., McCormick A. V., and Eisele F. L. (2008): Dependence of nucleation rates on sulfuric acid vapor concentration in diverse atmospheric locations, J. Geophys. Res., 113, D10209.

Kulmala M., Kontkanen J., Junninen H., Lehtipalo K., Manninen H. E., Nieminen T., Petäjä T., Sipilä M., Schobesberger S., Rantala P., Franchin A., Jokinen T., Järvinen E., Äijälä M., Kangasluoma J., Hakala J., Aalto P. P., Paasonen P., Mikkilä J., Vanhanen J., Aalto J., Hakola H., Makkonen U., Ruuskanen T., Mauldin III R. L., Duplissy J., Vehkamäki H., Bäck J., Kortelainen A., Riipinen I., Kurtén T., Johnston M. V., Smith J. N., Ehn M., Mentel T. F., Lehtinen K. E. J., Laaksonen A., Kerminen V.-M., Worsnop D. R. (2013): Direct Observations of Atmospheric Aerosol Nucleation, Science, 339, 943-946.

Kumar, P. P., Broekhuizen K., and Abbatt J. P. D. (2003): Organic acids as cloud condensation nuclei: Laboratory studies of highly soluble and insoluble species, Atmos. Chem. Phys., 3, 509-520.

Lathem T. L., Beyersdorf A. J., Thornhill K. L., Winstead E. L., Cubison M. J., Hecobian A., Jimenez J. L., Weber R. J., Anderson B. E., and Nenes A. (2013): Analysis of CCN activity of Arctic aerosol and Canadian biomass burning during summer 2008, Atmos. Chem. Phys., 13, 2735-2756.

Martin M., Chang R. Y.-W., Sierau B., Sjogren S., Swietlicki E., Abbatt J. P. D., Leck C., and Lohmann U. (2011): Cloud condensation nuclei closure study on summer arctic aerosol, Atmos. Chem. Phys., 11, 11335-11350.

779 Moore R. H., Bahreini R., Brock C. A., Froyd K. D., Cozic J., Holloway J. S., Middlebrook
780 A. M., Murphy D. M., and Nenes A. (2011a): Hygroscopicity and composition of Alaskan
781 Arctic CCN during April 2008, Atmos. Chem. Phys., 11, 11807-11825.

782 Moore M. J. K., Furutani H., Roberts G. C., Moffet R. C., Gilles M. K., Palenik B., and
783 Prather K. A. (2011b): Effect of organic compounds on cloud condensation nuclei (CCN)
784 activity of sea spray aerosol produced by bubble bursting, Atmospheric Environment, 45,
785 7462-7469.

786 Ortega I. K., Suni T., Boy M., Grönholm T., Manninen H. E., Nieminen T., Ehn M., Junninen
787 H., Hakola H., Hellén H., Valmari T., Arvela H., Zegelin S., Hughes D., Kitchen M., Cleugh
788 H., Worsnop D. R., Kulmala M., and Kerminen V.-M. (2012): New insights into nocturnal
789 nucleation, Atmos. Chem. Phys., 12, 4297-4312.

790 Paramonov M., Aalto P. P., Asmi A., Prisle N., Kerminen V.-M., Kulmala M., and Petäjä T.
791 (2013): The analysis of size-segregated cloud condensation nuclei counter (CCNC) data and
792 its implications for cloud droplet activation, Atmos. Chem. Phys., 13, 10285-10301.

793 Park K., Kim G., Kim J.-s., Yoon Y.-J., Cho H.-j., and Ström J. (2014): Mixing State of Size-
794 Selected Submicrometer Particles in the Arctic in May and September 2012, Environ. Sci.
795 Technol., 48, 909-919.

796 Petters M. D. & Kreidenweis S. M. (2007): A single parameter representation of hygroscopic
797 growth and cloud condensation nucleus activity, Atmos. Chem. Phys., 7, 1961–1971.

798 Pruppacher H. R. & Klett J. D. (copyright 2010): Microphysics of Clouds and Precipitation,
799 Atmospheric and Oceanographic Sciences Library, Volume 18, ISBN 9780306481000,
800 Dordrecht: Springer Netherlands.

801 Rastak N., Silvergren S., Zieger P., Wideqvist U., Ström J., Svenningsson B., Maturilli M.,
802 Tesche M., Ekman A.M.L., Tunved P., and Riipinen I. (2014): Seasonal variation of aerosol
803 water uptake and its impact on the direct radiative effect at Ny-Ålesund, Svalbard, Atmos.
804 Chem. Phys., 14, 7445-7460.

805 Riipinen I., Sihto S.-L., Kulmala M., Arnold F., Dal Maso M., Birmili W., Saarnio K., Teinilä
806 K., Kerminen V.-M., Laaksonen A., and Lehtinen K. E. J. (2007): Connections between
807 atmospheric sulphuric acid and new particle formation during QUEST III–IV campaigns in
808 Heidelberg and Hyytiälä, Atmos. Chem. Phys., 7, 1899-1914.

Rogers R. R. & Yau M. K. (1996 reprint): A Short Course in Cloud Physics, 3rd edition, International Series in Natural Philosophy, 113, Butterworth-Heinemann an imprint of Elsvier, ISBN 0-7506-3215-1.

Rolph G. D. (2014): Real-time Environmental Applications and Display sYstem (READY) Website (http://ready.arl.noaa.gov). NOAA Air Resources Laboratory, Silver Spring, MD.

Rose D., Nowak A., Achtert P., Wiedensohler A., Hu M., Shao M., Zhang Y., Andreae M. O., and Pöschl U. (2010): Cloud condensation nuclei in polluted air and biomass burning smoke near the mega-city Guangzhou, China–Part 1: Size-resolved measurements and implications for the modeling of aerosol particle hygroscopicity and CCN activity, Atmos. Chem. Phys., 10, 3365-3383.

Shaw G. E. (1986): Cloud condensation nuclei associated with Arctic haze, Atmospheric Environment, 20, 1453-1456.

Silvergren S. Wideqvist U., Ström J., Sjogren S., and Svenningsson B. (2014): Hygroscopic growth and cloud forming potential of Arctic aerosol based on observed chemical and physical characteristics (a 1 year study 2007-2008), J. Geophys. Res. Atmos, 119, 14,080-14,097.

Sipilä M., Berndt T., Petäjä T., Brus D., Vanhanen J., Stratmann F., Patokoski J., Mauldin III R. L., Hyvärinen A.-P., Lihavainen H., and Kulmala M. (2010): The Role of Sulfuric Acid in Atmospheric Nucleation, Science, 327, 1243-1246.

Sullivan R. C., Moore M. J. K., Petters M. D., Kreidenweis S. M., Roberts G. C., and Prather K. A. (2009): Effect of chemical mixing state on the hygroscopicity and cloud nucleation properties of calcium mineral dust particles, Atmos. Chem. Phys., 9, 3303-3316.

Tunved P., Ström J., and Krejci R. (2013): Arctic aerosol life cycle: linking aerosol size distributions observed between 2000 and 2010 with air mass transport and precipitation at Zeppelin station, Ny-Ålesund, Svalbard, Atmos. Chem. Phys., 13, 3643-3660.

Yli-Juuti T., Nieminen T., Hirsikko A., Aalto P. P., Asmi E., Hõrrak U., Manninen H. E., Patokoski J., Dal Maso M., Petäjä T., Rinne J., Kulmala M., and Riipinen I. (2011): Growth rates of nucleation mode particles in Hyytiälä during 2003−2009: variation with particle size, season, data analysis method and ambient conditions, Atmos. Chem. Phys., 11, 12865-12886.

838 Yum S. S. & Hudson J. G. (2001): Vertical distributions of cloud condensation nuclei spectra
839 over the springtime Arctic Ocean, J. Geophys. Res., 106(D14), 15045-15052.

840 Zieger P., Fierz-Schmidhauser R., Gysel M., Ström J., Henne S., Yttri K. E., Baltensperger
841 U., and Weingartner E. (2010): Effects of relative humidity on aerosol light scattering in the
842 Arctic, Atmos. Chem. Phys., 10, 3875-3890.
843

844 Table 1. Measured diameters when CCN/CN = 0.25, 0.50 and 0.75 and corresponding
845 calculated κ values with Eq. (1)

	June		August	
	Activation diameter (nm)	κ	Activation diameter (nm)	κ
CCN/CN = 0.25	49	0.7	56	0.5
CCN/CN = 0.50	60	0.4	67	0.3
CCN/CN = 0.75	72	0.2	78	0.2

846

847 Table 2. Experimentally-derived mass fractions (Silvergren et al., 2014), densities ρ and κ_i
848 values for each component used for the total κ calculations (Rastak et al., 2014 and references
849 therein). Properties of ammonium sulphate were assumed for the inorganic fraction.

Component	Mass fraction (%) June	Mass fraction (%) August	ρ (kg m^{-3})	κ_i
inorganics	88	90	1770	0.53
more water-soluble organics	10	7	1560	0.27
less water-soluble organics	2	2	1500	0.10
elemental carbon	1	1	1800	0.00
				Total κ
June				0.5
August				0.5

850

851

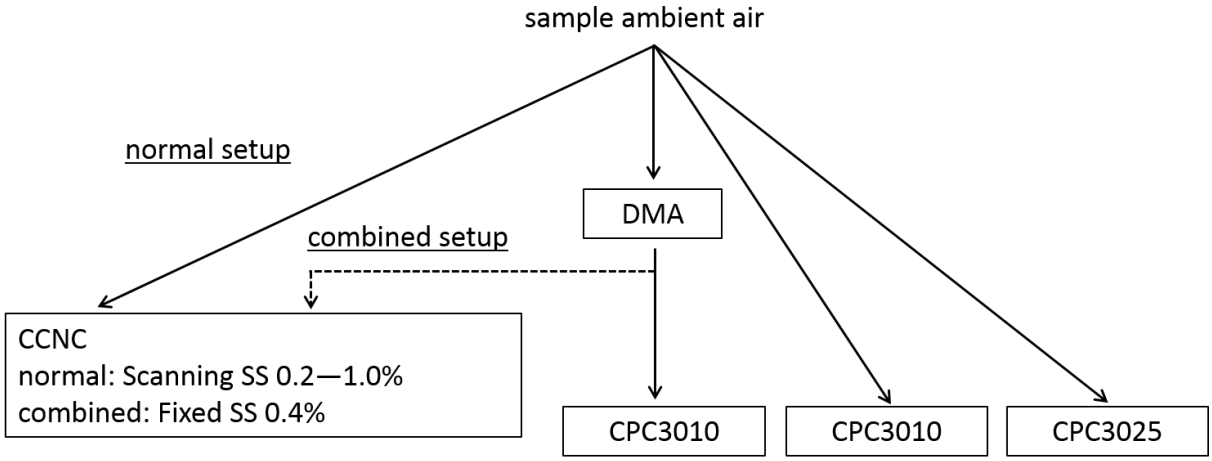

Figure 1. Scheme of the two different measurement modes for the cloud condensation nuclei counter (CCNC). When CCN size-resolved number concentration measurements took place, the CCNC was connected behind the Differential Mobility Analyzer and the supersaturation was set to 0.4%. During normal operation, the CCNC was connected parallel to the DMA and SS alternated between 0.2% and 1.0%.

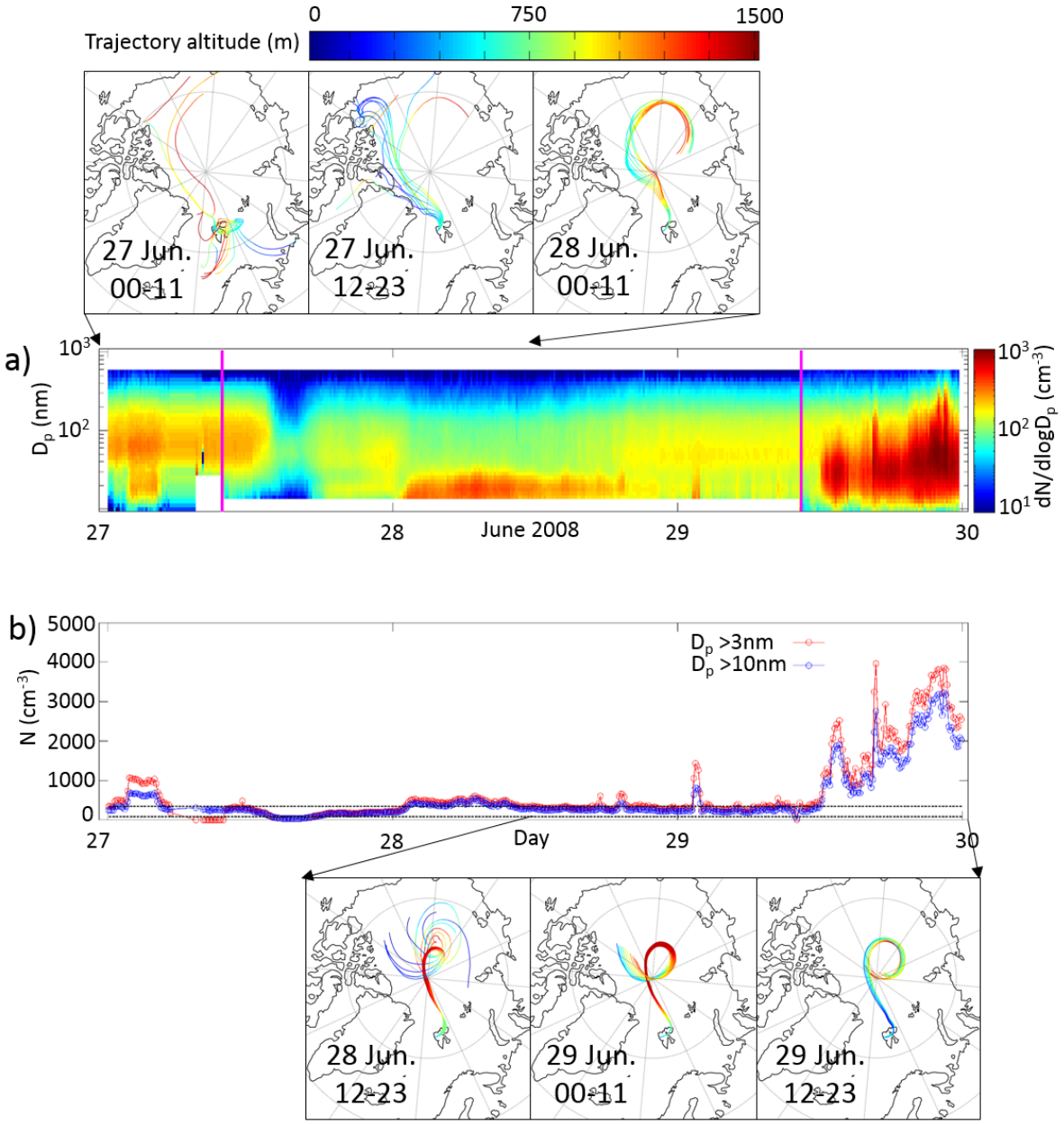

Figure 2. a) Particle number size concentration measured before, during, and after the size-resolved CCN concentration measurements were conducted in June 2008. Purple vertical lines indicate the start and end time of the CCN size-resolved concentration measurements. b) Time series of the 8-min medians from CPC measurements for the same period in June 2008. Horizontal dashed lines represent the 25th and 75th percentile of the CN number concentration for June during the years 2001 to 2010. Trajectory plots show 5-day backward trajectories, calculated for every hour. Trajectory plots on top of panel a) show air masses arriving between the 27 and midday of the 28 June at Zeppelin Research Station. Trajectory plots

below panel b) show air masses arriving between midday of the 28 June to midnight of the 29 June at Zeppelin Research Station.

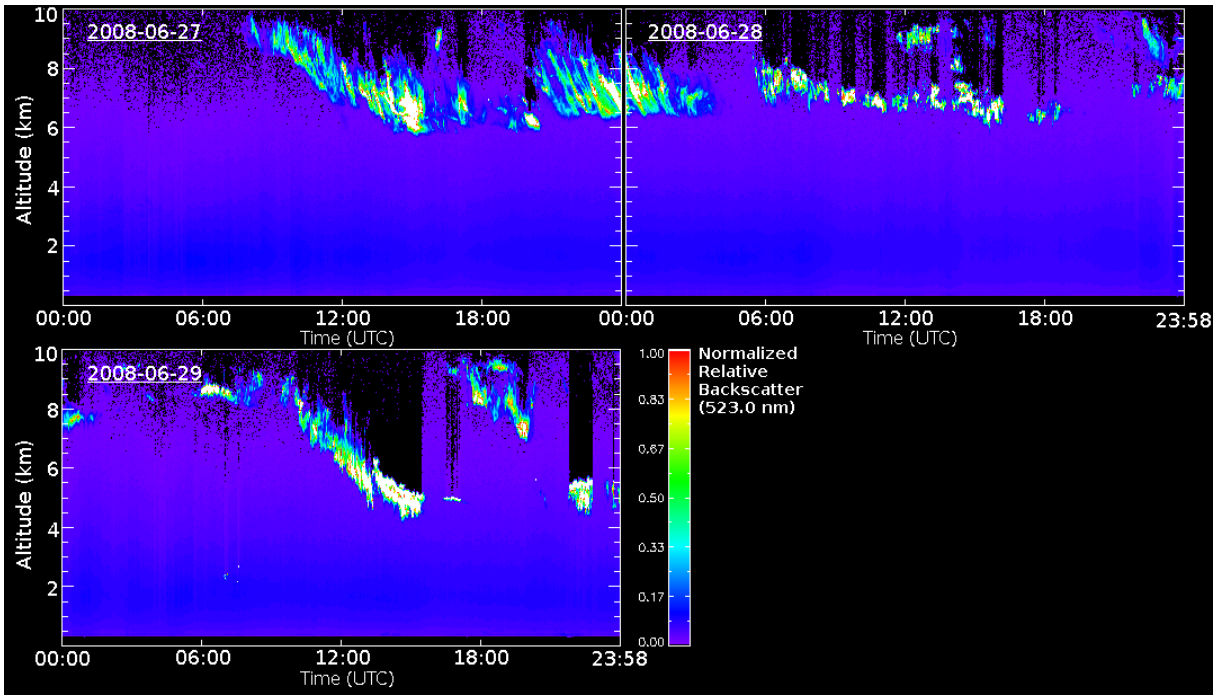

Figure 3. Normalized relative backscatter (Level 1.0 data) based on Lidar measurements at Ny-Ålesund recorded during the period 27–29 June 2008 (modified from http://mplnet.gsfc.nasa.gov/)

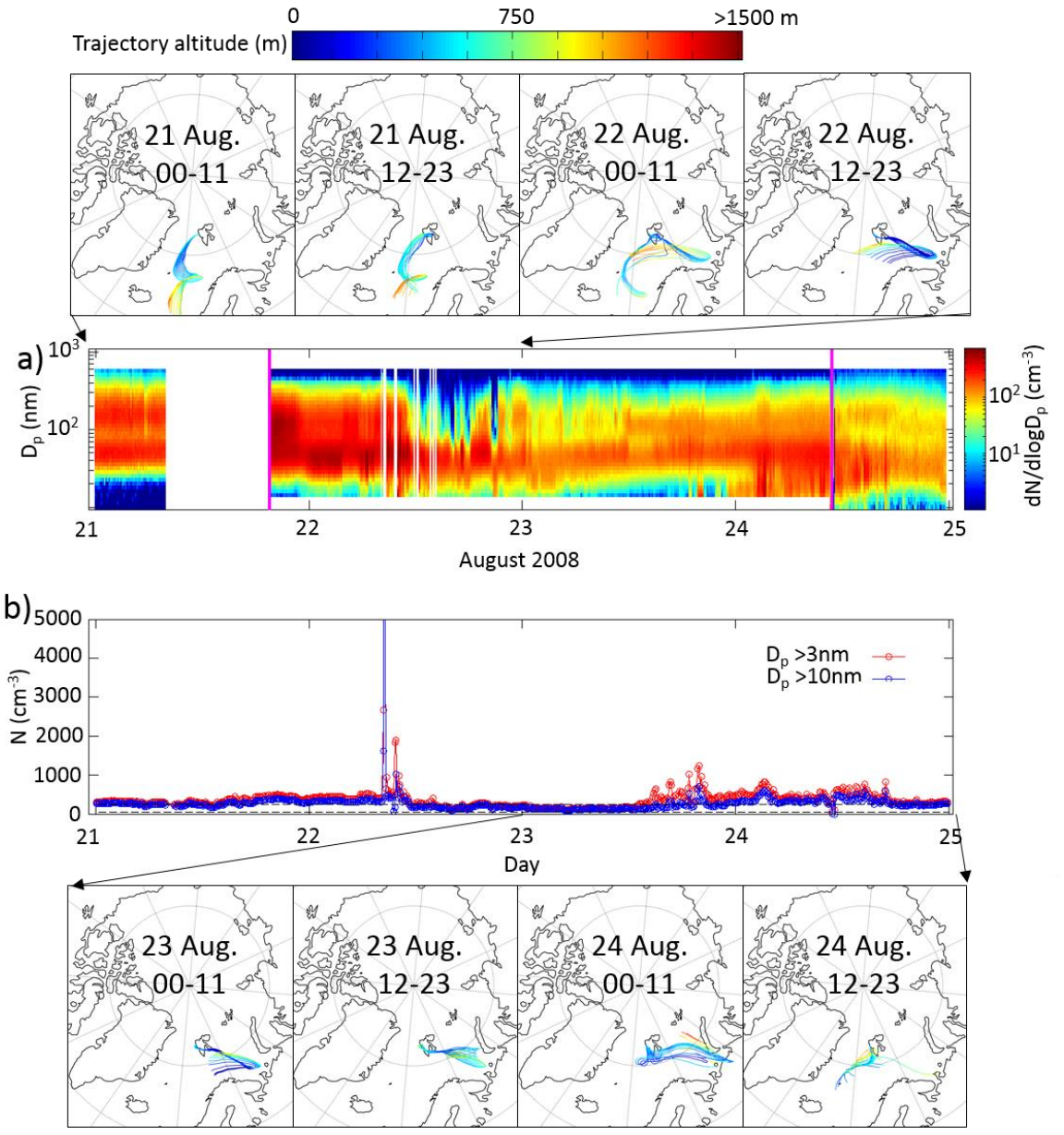

Figure 4. a) Particle number size concentration measured before, during, and after the size-resolved CCN concentration measurements were conducted in August 2008. Purple vertical lines indicate the start and end time of the CCN size-resolved concentration measurements. b) Time series of the 8-min medians from CPC measurements for the same period in August 2008. Horizontal dashed lines represent the 25th and 75th percentile of the CN number concentration for August during the years 2001 to 2010. Trajectory plots show 5-day backward trajectories, calculated for every hour. Trajectory plots on top of panel a) show air masses arriving between the 21 and 23 August 2008 at Zeppelin Research Station. Trajectory plots below panel b) show air masses arriving between midnight of the 23 August to midnight of the 24 August at Zeppelin Research Station.

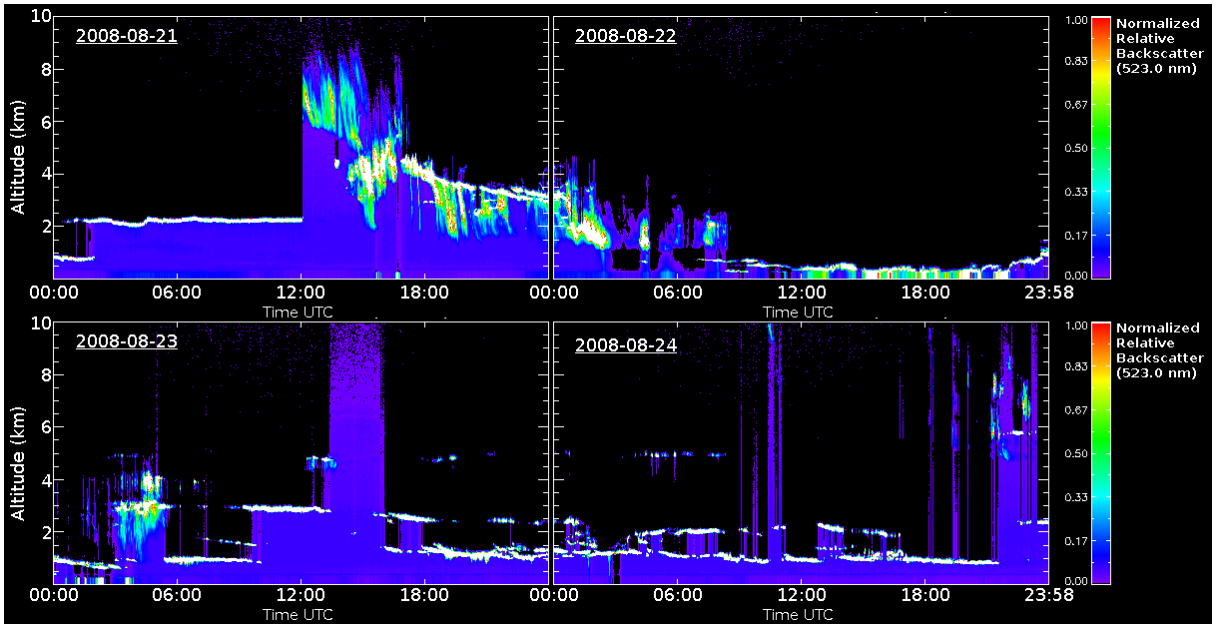

Figure 5. Normalized relative backscatter (Level 1.0 data) based on Lidar measurements at Ny-Ålesund recorded during the period 21–24 August 2008 (modified from http://mplnet.gsfc.nasa.gov/)

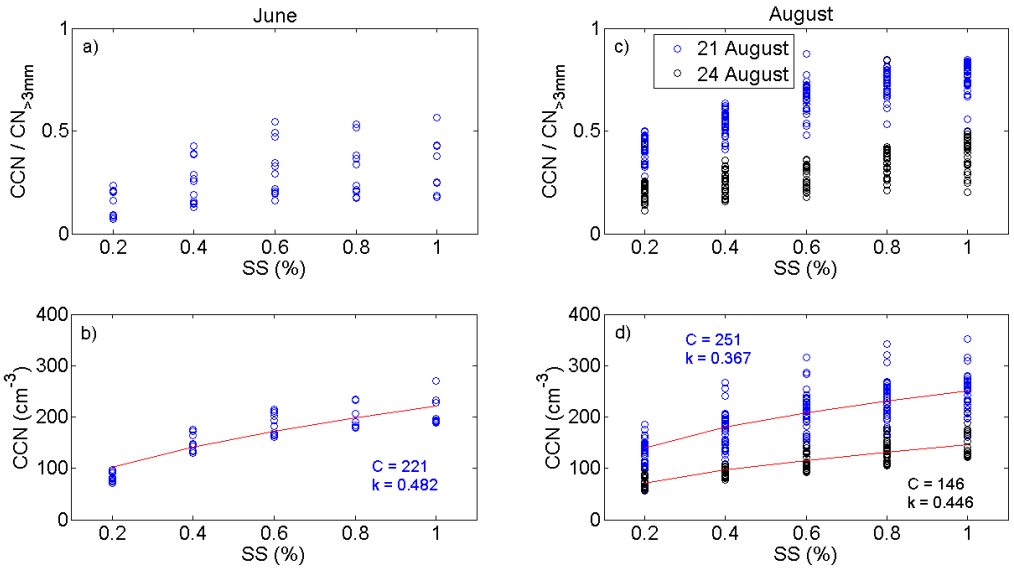

892

893 Figure 6. a) Ratios of the medians for each SS scan between CCN and particles with
894 diameters > 3nm ($CN_{>3nm}$) for June 2008 as a function of SS. b) Medians for each SS scan of
895 the total numbers of CCN as a function of SS for June 2008. c) Ratios of the medians for each
896 SS scan between CCN and particles with diameters > 3nm ($CN_{>3nm}$) for 21 and 24 August
897 2008 as a function of SS. d) Medians for each SS scan of the total numbers of CCN as a
898 function of SS for 21 and 24 August 2008. The red curves represent power-law function fits
899 to the data with the coefficients *C* and *k*.

900

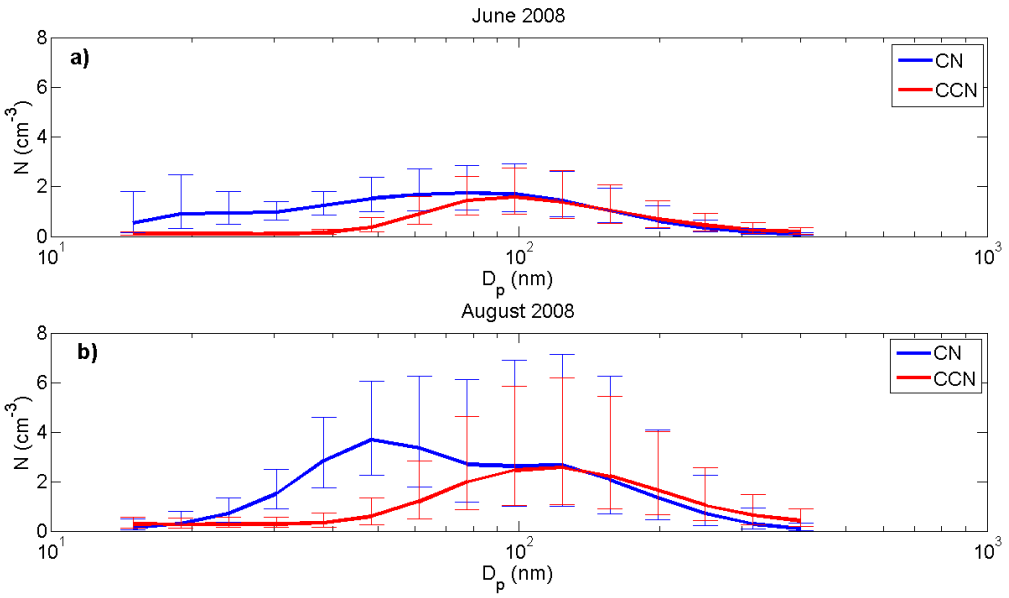

Figure 7. Geometric means of size-resolved particle density measurements and resulting CCN concentrations for the measurement period in a) June 2008 and b) August 2008. Measurements were conducted at 0.4% SS. Error bars indicate the geometric standard deviation.

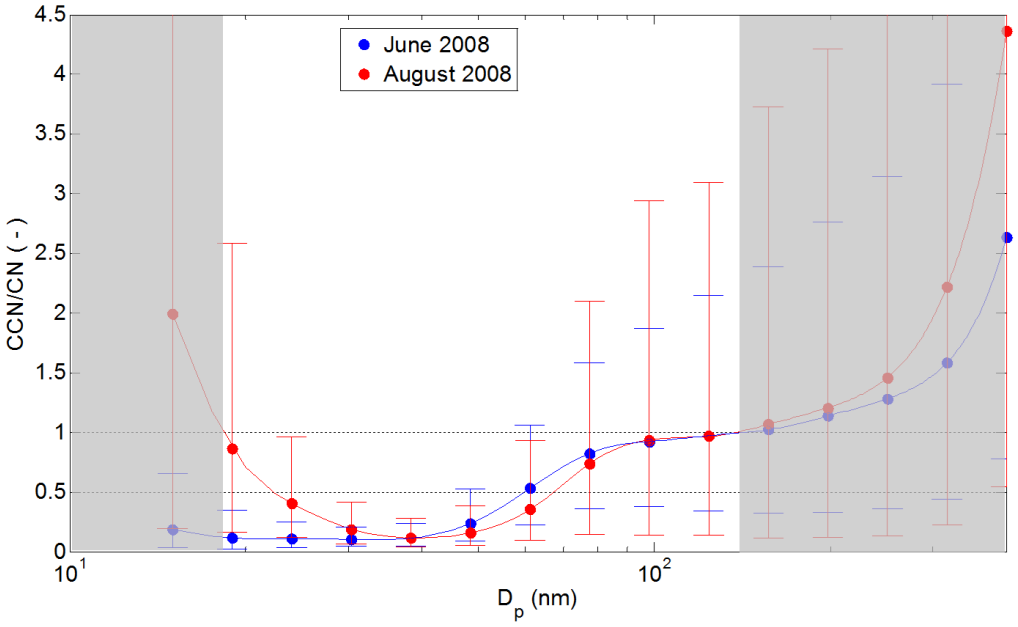

Figure 8. Activation ratio as a function of dry particle diameter (D_p) for the measurement period in June 2008 and August 2008. Obtained from measurements at a SS of 0.4%. Error bars indicate SD. The grey area indicates the for further analysis omitted data.